LARGE-GRAINED POLYCRYSTALLINE SILICON ON GLASS FOR THIN-FILM SOLAR CELLS

S. Gall *, J. Berghold, E. Conrad, P. Dogan, F. Fenske, B. Gorka, K. Lips,
M. Muske, K. Petter a), B. Rau, J. Schneider b), I. Sieber

Hahn-Meitner-Institut Berlin, Kekuléstr. 5, D-12489 Berlin, Germany
a) Now with: Q-Cells AG, Guardianstr. 16, D-06766 Thalheim, Germany
b) Now with: CSG Solar AG, Sonnenallee 1-5, D-06766 Thalheim, Germany
* Phone/Fax: +49-30-8062-1309/-1333, e-mail: gall@hmi.de

ABSTRACT: Large-grained polycrystalline silicon (poly-Si) films were prepared on glass using the 'seed layer concept' which is based on the epitaxial thickening of large-grained seed layers. The aluminium-induced layer exchange (ALILE) process was used to form p^+-type seed layers on glass. The seed layers feature a preferential (100) orientation of the grain surface. Epitaxial growth of the p-type absorber layers was carried out at temperatures § 600°C by either electron cyclotron resonance chemical vapour deposition (ECRCVD) or electron-beam evaporation. Secco etching was used to analyse extended defects in the films epitaxially grown on ideal substrates (Si wafers). Opposed to ECRCVD, films grown with electron-beam evaporation show no etch pits when deposited on Si(100) wafers. Post-deposition treatments (defect annealing and defect passivation) were used to improve the quality of the absorber layers. Thin-film solar cells were prepared on both Si(100) wafers (ideal seed layer) and seed layer covered glass substrates by the deposition of an n^+-type a-Si:H emitter and a TCO layer. The best solar cell results were achieved by electron-beam evaporation: $\eta = 1.3\%$ on seed layer covered glass and $\eta = 4.9\%$ on a Si(100) wafer.
Keywords: Polycrystalline, Silicon, Thin Film

1 INTRODUCTION

During the last years the world-wide production of solar cells has grown dramatically. With a share of more than 90%, the market is dominated by wafer-based crystalline silicon solar cells. In order to maintain the dramatic growth in the future significant cost reductions are required. It is expected that a transition from the well-established wafer-based crystalline silicon solar cells to high efficiency silicon thin-film solar cells on large-area glass substrates offers a high potential for such cost reductions. But, unfortunately, the existing silicon thin-film technologies based on hydrogenated amorphous Si (a-Si:H) and microcrystalline Si (µc-Si:H) suffer from their relatively low efficiencies (compared to the standard wafer-based solar cells). Thus, a new thin-film technology is required which provides silicon films on glass with material quality comparable to that of silicon wafers usually used by the photovoltaic industry. In principle, large-grained polycrystalline silicon (poly-Si) on glass featuring grain sizes much larger than the film thickness could offer such a high material quality. In this paper we describe the status of the development of a poly-Si thin-film solar cell on glass at the Hahn-Meitner-Institut Berlin. We have prepared the poly-Si films on glass using a two step process: Firstly a thin p^+-type poly-Si film (seed layer) is formed by aluminium-induced crystallisation (AIC) of amorphous Si (a-Si). Secondly this seed layer is used as a template for the epitaxial growth of a p-type absorber layer. After the poly-Si film formation post-deposition treatments (defect annealing and defect passivation) have been applied to improve the material quality. To complete the solar cell both an n^+-type a-Si:H emitter layer and a transparent conductive oxide (TCO) have been deposited. The schematic structure of the poly-Si thin-film solar cell is shown in Fig. 1. In the following sections results we obtained so far are presented.

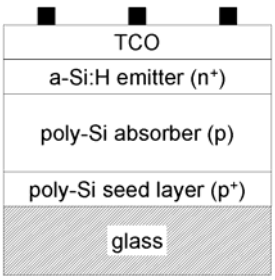

Figure 1: Schematic structure of a poly-Si thin-film solar cell on glass consisting of a p^+-type poly-Si seed layer, a p-type poly-Si absorber, an n^+-type a-Si:H emitter, a transparent conductive oxide (TCO), and metal contacts to both TCO and absorber (not shown here).

2 SEED LAYER FORMATION

The seed layers have been formed by the aluminium-induced layer exchange (ALILE) process which is based on aluminium-induced crystallisation of amorphous Si [1-3]. Starting point for the process is the following stack: glass/Al(300nm)/a-Si(375nm). For our experiments we have used either Corning 1737F or Schott Borofloat 33 glass substrates. Both layers (Al and a-Si) have been deposited in the same chamber by DC magnetron sputtering. The ALILE process requires a thin permeable membrane between the Al and the a-Si layer which controls the diffusion of Al and Si. The membrane (a thin Al oxide layer) has been formed by exposure to air of the Al-coated glass substrate (prior to the deposition of the a-Si layer). Annealing of the initial glass/Al/a-Si stack at temperatures below the eutectic temperature of the Al/Si system (T_{eu}=577°C) leads to a layer exchange and a concurrent crystallisation of Si. Finally a glass/poly-Si/Al(+Si) stack is formed (Fig. 2). The membrane stays in place during the entire ALILE process. Thus, the thickness of the resulting poly-Si film

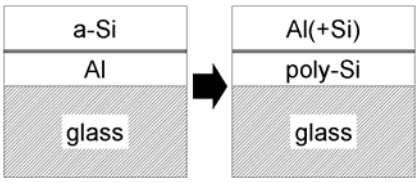

Figure 2: Schematic illustration of the aluminium-induced layer exchange (ALILE) process. During an annealing step the initial glass/Al/a-Si stack is transformed into a glass/poly-Si/Al(+Si) stack. The permeable membrane between the layers (grey line) stays in place during the ALILE process.

is determined by the thickness of the initial Al layer (300nm). The layer on top of the poly-Si film consists of Al and some Si inclusions ('Si islands').

The ALILE process starts with the diffusion of Si across the membrane into the Al layer. Upon supersaturation Si nuclei are formed within the Al layer. The growth of these nuclei is limited in vertical direction by both the glass substrate and the membrane at the initial Al/a-Si interface. However, in lateral direction the nuclei can grow until adjacent grains coalesce and finally form a continuous poly-Si film on the glass substrate. The process is characterised by self regulated suppression of nucleation by existing grains resulting in grain sizes above 10µm. More details about nucleation and growth during the ALILE process can be found in [4-6].

A characteristic feature of the seed layers prepared by the ALILE process is (besides the large grain sizes) the preferential (100) orientation of the grain surface. This is favourable for the epitaxial thickening of the seed layer at low temperatures. Up to about 75% of the area is tilted by less than 20° with respect to the perfect (100) orientation [7]. The preferential orientation depends on the annealing temperature and the way the membrane is formed [7, 8]. A theoretical model explaining the experimentally observed preferential (100) orientation of the seed layer grains has been proposed recently [9].

For the subsequent epitaxial growth on the poly-Si seed layer the membrane and the Al(+Si) layer have been removed by chemical mechanical polishing (CMP).

3 LOW-TEMPERATURE EPITAXY

We have studied the epitaxial growth of Si using both electron cyclotron resonance chemical vapour deposition (ECRCVD) and electron-beam evaporation. Due to the glass substrate the growth processes are limited to about 600°C. This temperature limit is very crucial to the epitaxial growth. In this section we describe mainly results obtained on monocrystalline Si wafers. The Si wafers act as a reference substrate to study the quality of the low-temperature epitaxy in detail.

The films grown by ECRCVD have been deposited decomposing silane (SiH_4) and diborane (B_2H_6) in a hydrogen (H_2) plasma. The base pressure was about $5x10^{-7}$mbar. The films were grown with a deposition rate of up to 20nm/min.

The electron-beam evaporation chamber is equipped with a 100cm^3 crucible for Si and a boron effusion cell. The base pressure was about $1x10^{-8}$mbar and the deposition rate was about 150nm/min.

Secco etch experiments have been used to determine the structural quality of the epitaxially grown films (HF(50%):0.15mol $K_2Cr_2O_7$ mixed 2:1). The samples were etched for 10s. Fig. 3 shows scanning electron microscopy (SEM) top view images of two Secco-etched films grown on Si(100) wafers. On the left hand side of Fig. 3, a surface of a Si film grown by ECRCVD is shown (film thickness: 1400nm, substrate temperature: 560°C, not intentionally doped). A large number of etch pits are visible. The etch pit density is about $5x10^8$cm^{-2}. A detailed description of the etch pits we have observed can be found in [7, 10]. The right hand side of Fig. 3 shows a surface of a Si film grown by electron-beam evaporation (film thickness: 840nm, substrate temperature: 600°C, not intentionally doped). No etch pits have been found. This reveals the high structural quality of the film. The structural quality of the grown film depends not only on the deposition technique but also on the crystallographic orientation of the underlying substrate. With ECRCVD we did not obtain epitaxial growth on Si(110) and Si(111) wafers. However, using electron-beam evaporation epitaxial growth has been achieved also on Si(110) and Si(111) wafers. The corresponding etch pit densities at a substrate temperature of 600°C are about $8x10^6$cm^{-2} and $2x10^8$cm^{-2}, respectively [11].

Using ECRCVD we have epitaxially thickened up to approximately 83% of the seed layer surface [7]. This has been reached because of the preferential (100) orientation of the seed layer. On the remaining seed layer surface fine-crystalline growth has taken place. In a different ECRCVD system our seed layers have been thickened epitaxially on the whole surface [12]. This means that the difficulties we have observed so far are not inherently connected to ECRCVD but related to our equipment or to the deposition parameters we have used. Using electron-beam evaporation we are able to grow epitaxially on the whole seed layer surface [11].

We have investigated the influence of boron doping on the effective doping level. The boron concentration in the films has been measured by secondary ion mass spectrometry (SIMS) and the resulting effective doping level has been determined using capacitance-voltage (C-V) measurements. The films grown by ECRCVD feature a big difference between the boron concentration and the effective doping level (the boron concentration is by

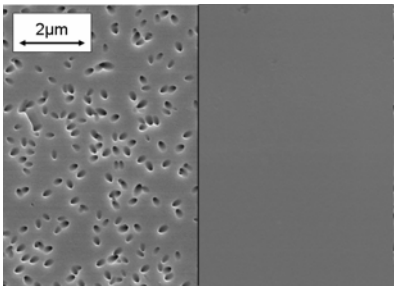

Figure 3: Scanning electron microscopy top view images of two Secco-etched sample surfaces. Left: Si film epitaxially grown by ECRCVD on a Si(100) wafer – a large number of etch pits are visible. Right: Si film epitaxially grown by electron-beam evaporation on a Si(100) wafer – no etch pits have been found.

about three orders of magnitude larger than the effective doping level) [7]. This is probably caused by a low doping efficiency (inactive boron atoms) and the compensation of the n-type behaviour usually observed for samples without boron doping. The films grown by electron-beam evaporation show only a small difference between the boron concentration and the effective doping level [13]. Thus, the effective doping level can be adjusted in a relatively simple way.

4 THIN-FILM SOLAR CELLS

Based on the film formation techniques described above silicon thin-film solar cells have been prepared. The basic structure of the solar cells is shown in Fig. 1. It consists of (1) a p^+-type poly-Si seed layer (about 200nm) prepared by the ALILE process, (2) a p-type poly-Si absorber (about 2000nm) grown by either ECRCVD or electron-beam evaporation, (3) an n^+-type a-Si:H emitter (about 20nm) deposited using plasma enhanced chemical vapour deposition (PECVD), and (4) a sputtered TCO window layer (about 80nm ZnO:Al). The emitter area has been defined by photolithography and subsequent wet-chemical mesa etching. After the mesa etching metal contacts (Al) have been prepared on both the TCO layer and the absorber layer (around the mesa). The shape of the metal contacts has also been defined by photolithography (using a lift off process). For comparison, Si thin-film solar cells have also been prepared on p^+-type Si(100) wafers (instead of the glass/ p^+-type poly-Si seed layer stack). The total area of the solar cells was 4mm x 4mm (the emitter area was either 0.122cm^2 or 0.086cm^2).

Post-deposition treatments (defect annealing and defect passivation) have been used to improve the quality of the solar cells. The treatments have been applied after the absorber layer deposition (prior to the emitter deposition). If both post-deposition treatments have been used the defect passivation step has taken place after the defect annealing step.

Defect annealing has been carried out by a very short 'high temperature step' (far above the deposition temperature of the absorber layer) either in a conventional tube furnace or in a rapid thermal processing (RTP) system. Different annealing temperatures and annealing durations have been used (850°C - 950°C; 200s – 400s). More information on the defect annealing we have applied can be found in [14]. A more detailed investigation about the influence of defect annealing on the open circuit voltage of poly-Si thin-film solar cells is given in [15].

The importance of defect passivation for poly-Si thin-film solar cells was impressively shown in [16]. They demonstrated that the module efficiency of poly-Si thin-film solar cells can be dramatically increased from less than 2% to more that 8% by a rapid, high-temperature (around 610°C), remote-plasma hydrogenation process. We have carried out defect passivation by hydrogenation in a parallel-plate PECVD system at 350°C for 15min (the PECVD system has also been used for the n^+-type a-Si:H emitter deposition). The PECVD system we have used limits the maximum temperature to 350°C.

The application of our post-deposition treatments, which are not yet optimised, has led to an efficiency increase of our ECRCVD grown poly-Si thin-film solar cells on glass by 95% (defect annealing) and 245% (defect annealing and defect passivation) with respect to the as-grown efficiency.

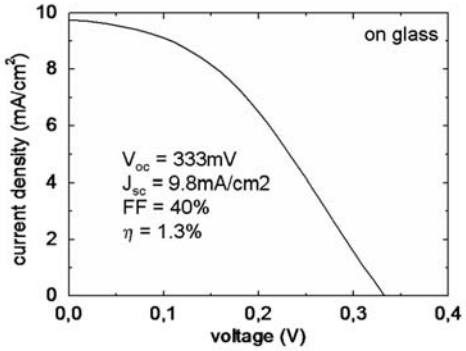

Figure 4: Current density versus voltage of a Si thin-film solar cell under illumination (AM1.5, 100mW/cm^2, 25°C). The absorber of the solar cell was grown on a p^+-type poly-Si seed layer on glass by electron-beam evaporation. For the analysis the area of the emitter layer has been used (0.086cm^2).

Using ECRCVD, the best solar cell on glass features an efficiency of η = 1.1% (an open circuit voltage of V_{oc} = 386mV, a short circuit current density of J_{sc} = 6.2mA/cm^2, and a fill factor of FF = 46%). In this paper all area-related results (e.g. efficiency) have been calculated using the emitter area, not the total area. The best results obtained so far using ECRCVD are V_{oc} = 397mV and J_{sc} = 6.7mA/cm^2. On Si(100) wafers the best cell shows an efficiency of η = 4.2% (V_{oc} = 458mV, J_{sc} = 13.0mA/cm^2, FF = 71%). So far the maximum values are V_{oc} = 498mV and J_{sc} = 13.8mA/cm^2.

The best results on both glass and Si(100) wafers have been achieved using electron-beam evaporation. The corresponding current-voltage characteristics under illumination (AM1.5, 100mW/cm^2, 25°C) are shown in Fig. 4 (on glass) and Fig. 5 (on Si(100) wafer). So far we have achieved efficiencies of 1.3% on glass (V_{oc} = 333mV, J_{sc} = 9.8mA/cm^2, FF = 40%) and 4.9% on Si(100) wafers (V_{oc} = 564mV, J_{sc} = 11.6mA/cm^2, FF =

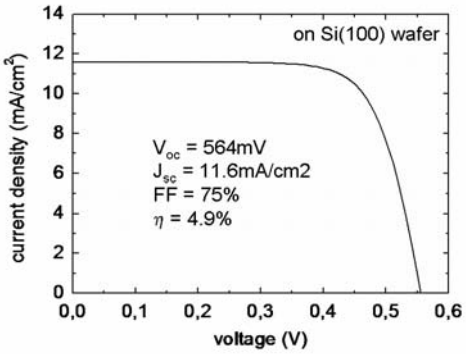

Figure 5: Current density versus voltage of a Si thin-film solar cell under illumination (AM1.5, 100mW/cm^2, 25°C). The absorber of the solar cell was grown on a p^+-type Si(100) wafer by electron-beam evaporation. For the analysis the area of the emitter layer has been used (0.122cm^2).

75%). The results for V_{oc} and J_{sc} on glass mentioned before are the maximum values. On Si(100) wafers the maximum values for V_{oc} and J_{sc} are 577mV and 11.9mA/cm^2, respectively.

The results we have obtained so far are somewhat lower than results recently published for more or less the same cell concept (epitaxial thickening of an ALILE seed layer by ion-assisted deposition) [17].

It is expected that the solar cells results can be improved dramatically by the optimisation of the processes we have used (seed layer formation, epitaxial growth of the absorber layer, post-deposition treatments, and solar cell preparation). The huge potential of such optimisations was already demonstrated for the defect passivation step [16].

5 SUMMARY AND CONCLUSIONS

Large-grained poly-Si thin films have been prepared on glass using the 'seed layer concept'. The seed layers have been formed by the ALILE process. They are characterised by a large grain size and a preferential (100) orientation of the grains. The seed layers have been epitaxially thickened by either ECRCVD or electron-beam evaporation. The structural quality of films epitaxially grown on Si wafers has been investigated by Secco-etch experiments. Films grown by electron-beam evaporation on Si(100) wafers feature no etch pits. Thin-film solar cells have been prepared on both seed layer covered glass and Si(100) wafers. The best solar cell results have been achieved using electron-beam evaporation. We have achieved efficiencies of 1.3% on glass and 4.9% on Si(100) wafers.

The potential of large-grained poly-Si thin-film solar cells on glass for efficiencies comparable to that of standard wafer-based Si solar cells has not been demonstrated so far. Although a strong improvement of the solar cell results is expected in the near future it is still an open question whether such high efficiencies can finally be reached. Strong research efforts are required to answer this question.

6 ACKNOWLEDGEMENTS

This work was partly funded by the European Commission under project number ENK5-CT-2001-00543 ('METEOR'). The authors would like to thank K. Jakob, C. Klimm, and T. Weber from HMI for technical assistance during sample preparation.

7 REFERENCES

[1] O. Nast, T. Puzzer, L.M. Koschier, A.B. Sproul, S.R. Wenham, Applied Physics Letters 73 (1998) 3214.

[2] O. Nast, S.R. Wenham, Journal of Applied Physics 88 (2000) 124.

[3] O. Nast, A.J. Hartmann, Journal of Applied Physics 88 (2000) 716.

[4] J. Schneider, J. Klein, M. Muske, S. Gall, W. Fuhs, Applied Physics Letters 87 (2005) 031905-1.

[5] J. Schneider, J. Klein, A. Sarikov, M. Muske, S. Gall, W. Fuhs, Materials Research Society Symposium Proceedings 862 (2005) A2.2.1.

[6] J. Schneider, A. Schneider, A. Sarikov, J. Klein, M. Muske, S. Gall, W. Fuhs, Journal of Non-Crystalline Solids 352 (2006) 972.

[7] S. Gall, J. Schneider, J. Klein, K. Hübener, M. Muske, B. Rau, E. Conrad, I. Sieber, K. Petter, K. Lips, M. Stöger-Pollach, P. Schattschneider, W. Fuhs, Thin Solid Films 511-512 (2006) 7.

[8] H. Kim, D. Kim, G. Lee, D. Kim, S.H. Lee, Solar Energy Materials & Solar Cells 74 (2002) 323.

[9] J. Schneider, A. Sarikov, J. Klein, M. Muske, I. Sieber, T. Quinn, H.S. Reehal, S. Gall, W. Fuhs, Journal of Crystal Growth 287 (2006) 423.

[10] K. Petter, D. Eyidi, M. Stöger-Pollach, I. Sieber, P. Schubert-Bischoff, B. Rau, A.T. Tham, P. Schattschneider, S. Gall, K. Lips, W. Fuhs, Physica B 376-377 (2006) 117.

[11] B. Gorka, P. Dogan, I. Sieber, F. Fenske, S. Gall, Thin Solid Films (2006), submitted.

[12] G. Ekanayake, T. Quinn, H.S. Reehal, B. Rau, S. Gall, Proceedings of the 21st European Photovoltaic Solar Energy Conference, Dresden, Germany (2006), this conference.

[13] P. Dogan, B. Gorka, I. Sieber, F. Fenske, S. Gall, Proceedings of the 21st European Photovoltaic Solar Energy Conference, Dresden, Germany (2006), this conference.

[14] B. Rau, E. Conrad, S. Gall, Proceedings of the 21st European Photovoltaic Solar Energy Conference, Dresden, Germany (2006), this conference.

[15] M.L. Terry, A. Straub, D. Inns, D. Song, A.G. Aberle, Proceedings of the 31st IEEE Photovoltaic Specialists Conference, Lake Buena Vista, Florida, USA (2005) 971.

[16] M.J. Keevers, A. Turner, U. Schubert, P.A. Basore, M.A. Green, Proceedings of the 20th European Photovoltaic Solar Energy Conference, Barcelona, Spain (2005) 1305.

[17] A.G. Aberle, Proceedings of the 4th World Confrence on Photovoltaic Energy Conversion, Waikoloa, Hawaii, USA (2006), in press.